



Contents lists available at ScienceDirect



Mechanism and Machine Theory

journal homepage: www.elsevier.com/locate/mechmachtheory



Research paper

Kinematic performance evaluation of high-speed Delta parallel robots based on motion/force transmission indices

J. Brinker^a, B. Corves^a, Y. Takeda^{b,*}

^a Institute of Mechanism Theory, Machine Dynamics and Robotics, RWTH Aachen University, Kackertstraße 16–18, Aachen 52072, Germany

^b Department of Mechanical Engineering, Tokyo Institute of Technology, 2-12-1, Ookayama, Meguro-ku, Tokyo 152-8552, Japan

ARTICLE INFO

Article history:

Received 7 October 2017

Revised 27 November 2017

Accepted 29 November 2017

Available online 2 February 2018

Keywords:

Delta parallel robots

Kinematics

Motion/force transmissibility

Constrainability

ABSTRACT

Motion and force transmission indices are a common measure for the kinematic performance analysis and optimization of parallel manipulators. However, a separate consideration of the constraint characteristics is inevitable for the analyses of limited-dof parallel manipulators. Such separation may distort the performance evaluation as the design parameters of parallel manipulators are highly coupled. In this context, different formulations for the transmissibility and constrainability of parallel manipulators based on the notion of power coefficients and pressure angles are revisited and applied to the performance evaluation of a non-overconstraint Delta robot, a well-known lower-dof parallel robot. Following the concept of pressure angles, a physically meaningful measure is proposed, which aggregates the transmission and constraint characteristics into a single index. The simple definition does not require the tedious computation of the normalization factor as used for power coefficients. Moreover, the applicability of the different formulations for the performance evaluation and optimization is critically discussed revealing insights into the particularities of the different indices and their interactions as well as proving the validity of the new approach.

© 2017 Elsevier Ltd. All rights reserved.

1. Introduction

Highly dynamic handling tasks require a high payload-to-weight ratio, a high positioning accuracy as well as excellent stiffness characteristics. Parallel manipulators meet these requirements by their architecture with frame-based actuation and thus low moving masses. The most widely spread manipulators within the niche market of parallel robotics are the 6-dof Gough/Stewart platform [1,2] and the 4-dof Delta robot [3] as commonly used for highly dynamic flight or driving simulation and high-speed pick-and-place applications with light-weight objects, respectively. In recent years, the design of the latter has been modified significantly extending its field of application to handling tasks with up to six dof (e.g., assorting, tooling, or measuring tasks) and/or with heavy-weight objects (e.g., stacking or packing tasks). At the same time, the high degree of industrial automation has led to growing demands for efficient and sustainable robotics systems. While the power consumption of a single system is comparatively low, companies may employ thousands of robots [4]. In addition, economically friendly added value and green manufacturing have become an important selling point of modern industries in recent years. In this context, the reduction of peak power demands is highly important since utility companies and electricity suppliers commonly charge their key accounts based on their peak demands in order to be able to accommodate for which

* Corresponding author.

E-mail addresses: brinker@igmr.rwth-aachen.de (J. Brinker), takeda@mech.titech.ac.jp (Y. Takeda).

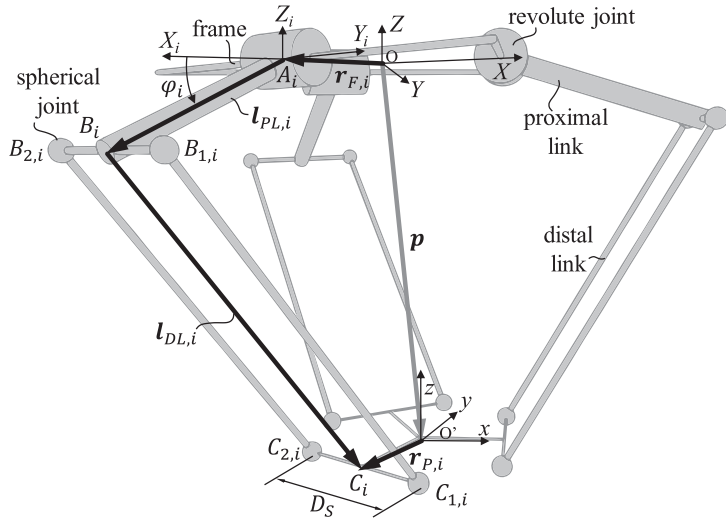


Fig. 1. Geometric relations of the 3-R(2-SS) Delta robot.

[5]. In a previous study [6], it was demonstrated that a purely kinematic design optimization of light-weight high-speed Delta parallel robots may be sufficient to obtain power efficient candidates for industrial application.

The main kinematic concepts for performance optimization are the concepts of condition number, manipulability, and motion/force transmissibility. Both measures the condition number as well as the manipulability are based on the characteristics of the Jacobian. In order to overcome the related problems of inhomogeneity and frame dependency, research has focused on alternative performance measures assessing the quality of motion and force transmission of parallel robots.

Against this background, existing approaches for the derivation of the input/output transmission and constraint characteristics, based on the virtual power coefficient and pressure angles, are reviewed. Taking advantage of the architecture of the Delta robot, in which six links are connected to the platform by spherical joints, a simple definition of the output transmission index is proposed. The proposed index is compared to other definitions for the output transmissibility and critically discussed with respect to its interaction with other measures, such as input transmission and constraint characteristics. Finally, a case study reveals the particularities of the proposed index for design optimization tasks.

2. Delta parallel robot

The Delta robot is one of the best known and most widely spread parallel robots in academia and industry [3]. The architecture is represented by three symmetric kinematic chains of different types (cf. Section 2.2), whereas industrial variants usually comprise of a rotationally actuated proximal link and a spatial parallelogram with four spherical joints and four links pairwise of the same length. With this design, the connecting rods only need to transmit axial forces allowing for light-weight design. In other variants, the spherical joints are replaced by universal joints in order to suppress the internal mobilities (i.e., the rotation of the rods along their axes of symmetry) that do not contribute to the output motion. Fig. 1 shows the schematic representation of the Delta robot and the related kinematic relations. Hereafter, R, U and S stands for revolute, universal and spherical joints, respectively, while an underlined symbol represents an actuated joint.

2.1. Geometric relations

The translational fully parallel Delta robot is characterized by spatial parallelograms (in which the two parallel connecting rods are denoted as distal link in the following) connecting the actuated proximal link to the moving platform. The platform position is denoted by \mathbf{p} . The positions of the actuated joints A_i at the frame and the connecting joints C_i at the platform can be expressed by the vectors $\mathbf{r}_{F,i}$ and $\mathbf{r}_{P,i}$, respectively. The vectors $\mathbf{l}_{PL,i}$ and $\mathbf{l}_{DL,i}$ point along the proximal and distal links of the i -th kinematic chain with $i = \{1, 2, 3\}$, cf. Fig. 1.

2.2. Mobility analysis

Translational parallel manipulators generally consist of three identical kinematic chains arranged symmetrically around a base. The general architecture of such chain can descriptively be represented by five revolute joints, where groups of two and three joint axes must be parallel [7]. The number of overconstraints of a Delta robot variant is depending on the geometric conditions within and among the chains. Thus, in the following, potential variants are evaluated in respect of their transmission and in particular constraint characteristics.

A simple form of a Delta kinematic chain is given as RUU, in which two pairs of revolute joints with orthogonal axes form two universal joints. Using three of these chains, the platform is supported by

- Three pure transmission forces (zero pitch wrenches) along the connecting rods and
- Three pure constraint moments (infinite pitch wrenches) along the common perpendicular to the universal joints' axes [8].

The resulting manipulator 3-RUU is sufficiently constrained and thus fulfils the general mobility criterion

$$M_{3-\text{RUU}} = 6(n - g - 1) + \sum_{q=1}^g f_q = 6(14 - 15 - 1) + 15 = 3 \quad (1)$$

with the number of bodies n , the number of kinematic pairs g , and the dof of the q th joint f_q . However, it is very prone to clearances resulting in parasitic motions of the platform [7]. In addition, the connecting rods are subject to bending and torsional moments.

Commercial Delta parallel robots are thus equipped with parallelograms increasing the stiffness properties while, in particular designs, only axial forces need to be transmitted by the connecting rods. A parallelogram is also referred to as single-closed-loop kinematic chain, composite pair, or complex joint. Such joint may comprise a 2-SS, 2-US, or 2-UU spatial four-bar linkage as well as a 2-RR planar linkage assembled with two revolute joints, also denoted as RPaR [9].

In the variant 3-R(2-SS), a spatial parallelogram is formed by four spherical joints and four links pairwise of the same length. As with the 3-RUU, it is sufficiently constrained requiring perfect manufacturing and assembly accuracies. In this case, the platform is supported by

- Three pure transmission forces (zero pitch wrenches) along the connecting rods and
- Three pure constraint moments (infinite pitch wrenches) perpendicular to the planes of the respective parallelograms [9–11].

For the mobility analysis of the 3-R(2-SS) Delta robot, the modified Chebyshev-Grübler-Kutzbach formula needs to be applied in order to take into account the six internal mobilities or idle dof κ (i.e., the rotations of the rods along their axes of symmetry) which do not contribute to the translational motion of the output link [9]:

$$M_{3-\text{R}(2-\text{SS})} = 6(n - g - 1) + \sum_{q=1}^g f_q - \kappa = 6(11 - 15 - 1) + 39 - 6 = 3 \quad (2)$$

The idle motions can be suppressed by replacing the complex 2-SS joint with the kinematically equivalent linkage 2-US [9]. Alternatively, bars or springs are commonly attached to the connecting rods by revolute joints, which at the same time maintains the coupling of socket and ball. The risk of parasitic motions of the non-overconstrained variant can be reduced by replacing all 12 spherical joints with universal joints. The resulting 3-R(2-UU) is overconstrained. Thus, the stiffness and load characteristics may be enhanced. Manufacturing and assembly inaccuracies may however lead to internal forces and even blocking of motion. The wrench system of the 3-R(2-UU) is provided by

- Three pure transmission forces (zero pitch wrenches) along the connecting rods and
- Six constraint moments (infinite pitch wrenches), where the directions of three couples are parallel to the platform and base (XY-plane) and the directions of the remaining three couples point in the direction perpendicular to the platform and base (Z-direction). Lying on a plane, the first group can be represented by two infinite pitch wrenches, leading to one overconstraint. Pointing in the same directions, the second group can be represented by a single infinite pitch wrench, resulting in another two overconstraints [9,11]. Furthermore, each parallelogram is subject to one overconstraint [10].

The mobility of the overconstrained manipulator can finally be derived by adding the number of overconstraints assembling the kinematic chains to a parallel manipulator (v_{PM}) and within the complex joints (v_{CJ}), i.e., $v = v_{PM} + v_{CJ} = 6$, to the mobility criterion, which gives

$$M_{3-\text{R}(2-\text{UU})} = 6(n - g - 1) + \sum_{q=1}^g f_q + v - \kappa = 6(11 - 15 - 1) + 27 + 6 - 0 = 3 \quad (3)$$

It should be noted that this variant is kinematically equivalent to the 3-R(RPaR) variant, in which a 2-RR planar linkage is utilized by adding two revolute joints to its connecting points. In this variant however each parallelogram is subject to three overconstraints ($v_{CJ} = 9$), which gives

$$M_{3-\text{R}(\text{RPaR})} = 6(n - g - 1) + \sum_{q=1}^g f_q + v - \kappa = 6(17 - 21 - 1) + 21 + 12 - 0 = 3 \quad (4)$$

Table 1 summarizes the mobilities for the different chain designs.

For industrial applications, the variants 3-R(2-SS) with additional springs and 3-R(RPaR) are prevalent. The following analyses are concerned with the 3-R(2-SS) variant.

Table 1
Mobilities of Delta-like robots depending on the kinematic chain design.

Kin. chain design					
Variant	3-RRU	3-R(2-SS)	3-R(2-US)	3-R(2-UU)	3-R(RPaR)
n	14	11	11	11	17
g	15	15	15	15	21
Σf_q	15	39	33	27	21
v_{CJ}	0	0	0	3	9
v_{PM}	0	0	0	3	3
κ	0	6	0	0	0
M	3	3	3	3	3

3. Kinematic performance indices

Parallel manipulators can be optimized such that specified workspace requirements are met. These are e.g., that the reachable workspace covers a prescribed workspace (as close as possible) or that the volume of the reachable workspace is maximized [12]. Similarly, the space occupation can be taken into account [13]. Manipulators that were optimized by workspace and occupied space requirements only may however suffer from poor kinematic and dynamic characteristics. Thus, kinematic and dynamic performance measures are commonly taken into account for the optimization of manipulators. The main kinematic concepts for performance measurement are the concepts of condition number, manipulability, and motion/force transmissibility [14].

Both measures, the condition number as well as the manipulability, are based on the characteristics of the Jacobian. The condition number [15,16] is a local measure of the Jacobian-induced distortion of the motion and force transmission from the joint to the end-effector space and, depending on the underlying norm, may be interpreted as uniformity factor of the Jacobian mapping (i.e., directional uniformity of the manipulability ellipsoid) [17]. The product of the singular values of the Jacobian matrix corresponds to the volume of the so-called manipulability ellipsoid. However, information on the directionality get lost. Besides the volume of the manipulability ellipsoid, several physical interpretations can be found for the manipulability index, e.g., the ease of changing arbitrarily the pose of the moving platform [18], the average mobility of the moving platform over all directions [19], the capability to exert a twist [20], or the overall manipulator sensitivity to actuator displacements [21]. In respect of these different characteristics, optimization results depend on the underlying measure [22].

In addition, for translational and rotational dof of the moving platform, the Jacobian matrix contains inhomogeneous units and further modification, e.g., normalization [23,24] or separate analyses of position and orientation [21,25] is required. Moreover, for limited-dof manipulators (e.g., the translational Delta robot), in which the connectivity of each serial kinematic chain may not be equal to the mobility of its moving platform, the 3×3 -Jacobian mapping the input to the output velocities may not be sufficient to predict all possible singularities [26]. Finally, Jacobian-based indices are frame-dependent. As a result, the values of the indices vary with the choice of coordinates [27]. Further critical discussions and comparisons of the different measures can be found in e.g., [19,21–23,28,29].

To overcome the problem of inhomogeneity and frame dependency, the performance of parallel manipulators can alternatively be assessed analyzing the quality of motion and force transmission, which is introduced in the following.

3.1. Motion and force transmission indices

The transmission of a mechanism is generally characterized by the motion transmission from the input to the output and by the force transmission from the output to the input [30]. The concept of the transmission angle was initially proposed for planar mechanisms [31]. Yuan et al. [32] proposed transmission indices for spatial manipulators by using the virtual coefficient between the transmission wrench screw (TWS) and the output twist screws (OTS) [33]. The initial approach was then normalized by Sutherland and Roth [34] and further generalized by Tsai and Lee [35] taking into account a generalized transmission wrench screw (GTWS) and the related virtual coefficients to the input and output screw. Based on that Chen and Angeles [36] proposed the generalized transmission index (GTI). The three approaches can be distinguished by the different definitions of the maximum value of the virtual coefficient (as used for normalization).

Takeda and Funabashi [37] proposed a transmission index (TI) for fully parallel manipulators taking into account the virtual power transmitted from the input links to the output link. Fixing all input links of a mechanism except one, single-dof mechanisms are generated and analyzed in respect of the pressure angles at the connection between the freed input link and the output. The concept represents a special case of the GTI when the TWS degenerates to a transmission force line (i.e., a zero-pitch TWS). In this case, the TWS can be defined at a (spherical) joint where no moment is applied as constraint resulting in a simple definition of the pressure angle. The approach was extended to cable driven parallel

mechanism [38] and spherical parallel mechanism [39]. Briot et al. [40] investigated the determination of the maximum reachable workspace of planar parallel manipulators based on the transmission angle and the position of the instantaneous center of rotation. Taking into account the output link's load condition, Shimojima et al. [41] proposed a unique definition of TWS.

In recent years, Wang et al. [42] consolidated the concept of virtual coefficient and Takeda's approach of fixing all inputs except one and proposed a general procedure for non-redundant spatial parallel manipulators. Using the notion of power coefficient, i.e., the normalized virtual coefficient, two indices are proposed in order to evaluate the transmission characteristics, i.e., the input transmission index (*ITI*) and output transmission index (*OTI*), where the minimum of both is denoted as local transmission index (*LTI*). The concept was extended for redundant and/or overconstrained parallel manipulators [43,44].

The larger the values of the proposed transmission indices, the better is the corresponding kinematic performance. Values close to zero correspond to near-singular configurations of the system. In this context, Gosselin and Angeles [16] distinguish between direct and inverse kinematic singularities when the Jacobians of the input and/or output, respectively, degenerate. In this case, the Jacobians lose rank, i.e., their determinants go zero. In a direct or forward kinematic singular configuration (also known as type I singularity), the robot loses one or more dof. In an inverse kinematic singular configuration (also known as type II singularity), the robot gains one or more dof. The case when both matrices are singular is termed combined singularity (also known as type III singularity) [16,45,46]. It should be noted that there exist many other definitions and classifications of singularities in literature. Exhaustive overviews are for instance presented in [47,48]. For alternative purely geometric methodologies to analyze the singularities of parallel manipulators it is referred to [49–51].

Constraint singularities, a phenomenon firstly identified by Zlatanov et al. [52], are not detected by only considering the input-output relations [26,53]. This particularly applies to lower-mobility manipulators, in which the constraint wrench system may degenerate or become rank deficient, respectively. Then, the chains lose their ability to constrain the platform, which gains at least one additional dof. In fact, with the proposed indices it is possible to detect a manipulator's closeness to actuation (transmission) singularities, whereas the closeness to constraint singularities cannot be detected [54,55]. Thus, constraint transmission indices (*CTI*) were developed as shown in [54,56] and further refined and discussed extensively in [57]. At the same time, Liu et al. [58] proposed a novel approach for the derivation of the maximum value of the virtual coefficient for parallel mechanisms with 1-dof joints connecting the kinematic chains to the output link.

If a non-overconstrained output link is fully constrained, the constraint wrench system and the actuation wrench system must always span a 6-system. In this case the output link is fully constrained (or cannot move respectively) when all actuated joints are locked. If, however, the actuation wrench system becomes rank deficient while the constraint wrench system keeps its rank (i.e., stays a 3-system in this case), actuation singularities occur [54,49].

Following the aforementioned approaches, the transmissibility and constrainability of a lower-mobility translational manipulator such as the Delta robot may be derived from two virtual situations. For the *OTI*, all actuated joints except one are locked and the incremental change of the platform position is computed. In a figurative sense, a virtual joint is added to restrain the platform motion to purely translational dof. This in turn implies that constrainability is ensured for all configurations (which corresponds to the definition of the actuation singularity). Accordingly, the constraint singularities must be tackled by additional means, i.e., the *CTI*. In this case, all actuated joints are locked while one of the constraint moments is removed from the system. In other words, a virtual joint is added allowing the platform to move along an actually constrained direction.

In contrast to that, this contribution is concerned with a single index to assess both, the output transmissibility and constrainability. The index naturally stems from the general architecture of the 3-R(2-SS) Delta robot. Accordingly, the output motion is supported by six links, connected by spherical joints. Locking all the actuated joints and removing one of the supporting links, provides information on the real system behavior. Then, the working wrench acting on the output link by the removed link (one SS-chain) and the unconstrained motion by the other links (five SS-chains) at their connecting joints can be evaluated with the following advantages.

The resulting index can be traced back to the concept of pressure angles constituting a physically meaningful index. The simple definition does not require the tedious computation of the normalization factor. Moreover, the resulting aggregation of *OTI* and *CTI* into a single index is considered valuable for design optimization tasks, whereas the lack of distinguishability between the types of singularity is of minor importance in this context.

The basic concept was initially presented in [59] and used for a combined kinematic and dynamic dimensional synthesis of functionally extended Delta parallel robots with additional rotational dof in [6]. Moreover, it was employed for the transmission analyses of a 3-PRS lower-mobility parallel mechanism [60]. In the latter study, a kinematically equivalent mechanism is defined in order to make the supporting chains generate force constraints only.

3.2. Analyses of motion and force transmission indices based on power coefficients

The transmission and constraint characteristics of parallel manipulators can be assessed based on the notion of power coefficient. In general, the orthogonal product of a wrench and twist screw ($\$_{ws}$ and $\$_{ts}$) related to a body is called virtual coefficient and can be interpreted as instantaneous power caused by the wrench acting on the moving body [57]. The higher the virtual coefficient, the better is the kinematic performance or the less wrench is required to transmit power [58]. The

power coefficient is given as normalized virtual coefficient, i.e., [33,34]

$$\rho = \frac{|\hat{\mathbf{s}}_{TS} \circ \hat{\mathbf{s}}_{WS}|}{|\hat{\mathbf{s}}_{TS} \circ \hat{\mathbf{s}}_{WS}|_{max}} \quad (5)$$

where $\hat{\mathbf{s}}_{TS}$ and $\hat{\mathbf{s}}_{WS}$ denote a unit twist and a unit wrench screw, respectively. Following the general definition of a screw

$$\hat{\mathbf{s}} = \begin{bmatrix} \mathbf{s} \\ \mathbf{s}_0 \times \mathbf{s} + \lambda \mathbf{s} \end{bmatrix} \quad (6)$$

where \mathbf{s} denotes a unit vector along the screw axis and \mathbf{s}_0 a position vector in a reference coordinate system to an arbitrary point on the screw axis. The instantaneous linear velocity of any point on a rigid body (in this case the origin of the reference coordinate system) is given by the parallel and normal velocities to a single axis called instantaneous screw axis. In this case \mathbf{s} represents the angular velocity about the screw axis inducing the normal velocity. The pitch λ then relates the angular velocity, which by definition points along the screw axis, to the parallel velocity. Similarly and due to the reciprocity of force and velocity, the unit vector \mathbf{s} in a wrench represents a force along the axis inducing a moment in the origin of the reference frame. The pitch relates the initial moment acting on the rigid body parallel to the screw axis to this force. Using the pitch as conversion factor allows for a pure dependency of all components on \mathbf{s} . The virtual work can be expressed as inner or orthogonal product of twist and wrench [45,46]

$$\delta W = \dot{q}\rho(\hat{\mathbf{s}}_T \circ \hat{\mathbf{s}}_W) = \dot{q}\rho[(\lambda_T + \lambda_W)\cos(\alpha) - d\sin(\alpha)] \quad (7)$$

where \dot{q} and ρ represent the intensities of the unit twist and wrench and α denotes the acute angle between the corresponding screw axes. The minimum distance d between two skew lines is given by the common perpendicular of which. The theory of reciprocal screws states that if a wrench acts on a rigid body in such a way that no work is produced while the body is undergoing an infinitesimal twist, the two related screws are reciprocal [45]. To assess the quality of a transmission it is thus sufficient to neglect the intensities and define the virtual coefficient as follows

$$\eta = (\lambda_T + \lambda_W)\cos(\alpha) - d\sin(\alpha) \quad (8)$$

For better presentation and comparison, a normalized index ranging between zero and one is desired. Therefore, the maximum virtual coefficient is derived based on [30]. Imagine a right triangle with the side lengths $(\lambda_T + \lambda_W)$ and d , it follows with the cosine and sinus of the angle δ :

$$\lambda_T + \lambda_W = \sqrt{(\lambda_T + \lambda_W)^2 + d^2} \cdot \cos(\delta) \quad (9)$$

and

$$d = \sqrt{(\lambda_T + \lambda_W)^2 + d^2} \cdot \sin(\delta) \quad (10)$$

respectively. With (8) this gives

$$\begin{aligned} \eta &= \sqrt{(\lambda_T + \lambda_W)^2 + d^2} \cdot (\cos(\delta)\cos(\alpha) - \sin(\delta)\sin(\alpha)) \\ &= \sqrt{(\lambda_T + \lambda_W)^2 + d^2} \cdot \cos(\delta + \alpha) \leq \sqrt{(\lambda_T + \lambda_W)^2 + d_{max}^2} = \eta_{max} \end{aligned} \quad (11)$$

where d_{max} was recently redefined as the maximum of two potential orthogonal distances of a wrench and twist screw pair [58]. Imagine a wrench to be applied from a transmitting link (e.g., a coupler) to another link (e.g., an output link). Then, the application point A is defined as the centroid of the connecting joint between the two links (e.g., the mid-point on the rotational axis of a revolute joint or the sphere center of a spherical joint) [30,36]. The points on the transmission wrench screw (TWS) axis and output twist screw (OTS) axis, which are closest to A are denoted as transmission and output characteristic points C_w and C_t . The related general formulation of the normalization is however not needed for the assessment of the constrainability and transmissibility of the Delta parallel robot as shown in the following section. Application examples of the general definition of the maximum virtual coefficient can be found in [58] and [61]. Finally, the power coefficient ρ is the normalized virtual coefficient. Thus, with (8), (11) and (5), it follows

$$\rho = \frac{|(\lambda_T + \lambda_W)\cos(\alpha) - d\sin(\alpha)|}{\sqrt{(\lambda_T + \lambda_W)^2 + d^2}} \quad (12)$$

3.3. Input transmission index

Following the notion of the power coefficient, the input transmission characteristics of a Delta robot can be derived by simple kinematic relations. The two connecting rods j within a chain i solely transmit axial forces denoted by the unit

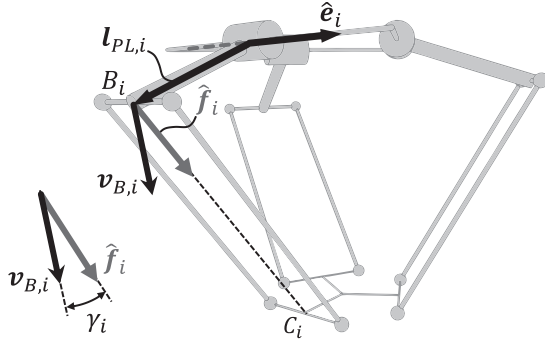


Fig. 2. Geometric relations: input transmission index.

vector $\hat{f}_{j,i}$. Hence, the direction of these forces is given by the vector \hat{f}_i (which corresponds to the normalized vector along the distal link $\mathbf{l}_{DL,i}$, cf. Fig. 1) providing a zero-pitch wrench screw with $\lambda_W = 0$. The axis of the zero-pitch ($\lambda_T = 0$) input twist screw (ITS) is given by the unit vector $\hat{\mathbf{e}}_i$ along the actuation axis. The vector along the proximal link is given by $\mathbf{l}_{PL,i}$, cf. Fig. 1. The power coefficient in A_i is then given as

$$\rho_i = \frac{|\mathbf{S}_{TWS,i} \circ \mathbf{S}_{ITS,i}|}{|\mathbf{S}_{TWS,i} \circ \mathbf{S}_{ITS,i}|_{\max}} = \frac{\left[\begin{array}{c} \mathbf{l}_{PL,i} \times \hat{f}_i \\ \hat{f}_i \end{array} \right]^T \left[\begin{array}{c} \hat{\mathbf{e}}_i \\ \mathbf{0}_3 \end{array} \right]}{|\mathbf{l}_{PL,i}|} = \frac{(\mathbf{l}_{PL,i} \times \hat{f}_i)^T \hat{\mathbf{e}}_i}{|\mathbf{l}_{PL,i}|} = (\hat{\mathbf{e}}_i \times \hat{\mathbf{l}}_{PL,i})^T \hat{f}_i \quad (13)$$

which corresponds to the angle between the velocity $\mathbf{v}_{B,i}$ of the spherical joint B_i and the direction of the force transmitted to the output link along the distal link. This angle can be interpreted as pressure angle γ_i of the input transmission. Its cosine value is thus

$$\lambda_{i,PA} = \cos(\gamma_i) = \mathbf{v}_{B,i}^T \hat{f}_i / \| \mathbf{v}_{B,i} \| \quad (14)$$

The relations are illustrated in Fig. 2. Accordingly, the best transmission occurs when the directions of velocity and force coincide. The input transmission index ITI is given as the minimum of the absolute pressure angles' cosine among all three kinematic chains, i.e.,

$$ITI = \min(|\lambda_{i,PA}|) \quad \forall i = \{1, 2, 3\} \quad (15)$$

For the derivation of the ITI based on the general definition in (12), it is useful to recapitulate the constraint wrench system of a revolute pair. It is represented by a 5-system composed of [62]:

- A restraint force along the axis of rotation
- A restraint force along the link (perpendicular to the axis of rotation), which can be represented by the linear combination of two restraint forces
- A restraint couple along the link, which can be represented by the linear combination of two restraint couples

Accordingly, the feasible twist of a revolute pair constitutes a 1-system represented by a zero-pitch screw. In other words, the constraint wrenches are reciprocal to the twist allowed by the revolute pair [36].

This also means that any moment applied to the tip of the proximal link about any wrench screw axis cannot be transmitted in a way that power is produced. It is thus sufficient to describe the transmission wrench by a so-called transmission force line (i.e., zero-pitch wrench). If both pitches vanish, the virtual coefficient is given as

$$\eta = \left[\begin{array}{c} \mathbf{s}_{0T} \times \mathbf{s}_T \\ \mathbf{s}_T \end{array} \right]^T \left[\begin{array}{c} \mathbf{s}_W \\ \mathbf{s}_{0W} \times \mathbf{s}_W \end{array} \right] = -ds \sin(\alpha) \quad (16)$$

where for the notations it is referred to (6). Defining the screw in the application point, it follows

$$\begin{aligned} \eta &= \mathbf{s}_W^T (\mathbf{s}_{0T} \times \mathbf{s}_T) + \mathbf{s}_T^T (\mathbf{s}_{0W} \times \mathbf{s}_W) = \hat{f}_i^T (\mathbf{0}_3 \times \mathbf{s}_T) + \hat{\mathbf{e}}_i^T (\mathbf{l}_{PL,i} \times \hat{f}_i) = \hat{f}_i^T (\hat{\mathbf{e}}_i \times \mathbf{l}_{PL,i} \hat{\mathbf{l}}_{PL,i}) \\ &= l_{PL,i} \hat{f}_i^T \hat{\mathbf{v}}_{B,i} = l_{PL,i} \cos(\gamma_i) \end{aligned} \quad (17)$$

with γ_i as pressure angle between the force and velocity. The power coefficient then is

$$\rho_i = \frac{-ds \sin(\alpha)}{d_{\max}} = \frac{l_{PL,i} \cos(\gamma_i)}{d_{\max}} = \cos(\gamma_i) \quad (18)$$

where the maximum distance is simply given by the length of the proximal link $d = d_{\max} = l_{PL,i}$.

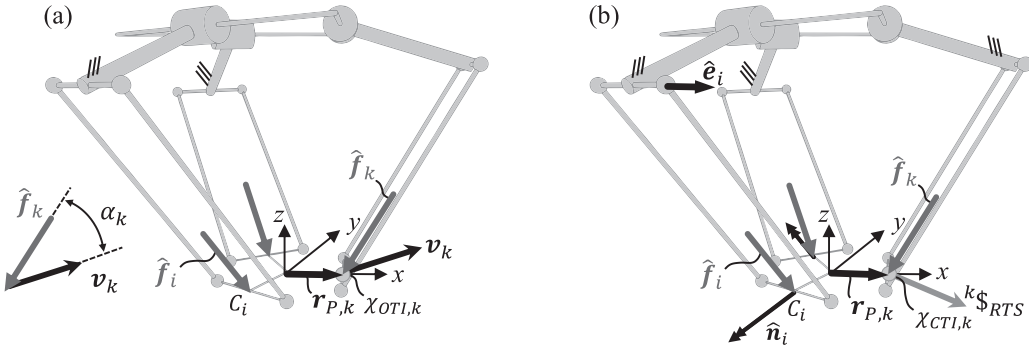


Fig. 3. Geometric relations: output and constraint transmission indices with three supporting links.

3.4. Output transmission index

The following analyses of the output transmission characteristics are divided into four parts deriving the output transmission index modeling the system with

- Three supporting links
- Three supporting links (including constraint characteristics)
- Six supporting links (general approach)
- Six supporting links (simplified approach)

As shown in [Section 2.2](#), the global wrench system of the 3-R(2-SS) Delta robot is a 6-system. The actuation wrench system is given by three pure transmission forces (zero pitch wrenches) along the connecting rods. The constraint wrench system includes three pure constraint moments (infinite pitch wrenches) perpendicular to the planes of the three parallelograms.

3.4.1. Three supporting links

Assume the platform to be well constrained by the architecture of the robot and imagine to fix all actuators or inputs except k , then the output link of the resulting single-dof mechanism performs a virtual translational motion [\[37\]](#). In this case, all transmission forces (given by the resultants of the rod forces of the parallelograms, [Fig. 3\(a\)](#)) except \hat{f}_k are constraint forces applying no work to the output link. The instantaneous motion of the output link is then given by

$${}^{(k)}\mathbf{S}_{OTS} = \begin{bmatrix} \mathbf{0}_3 \\ {}^{(k)}\mathbf{v}_i \end{bmatrix} \quad (19)$$

with ${}^{(k)}\mathbf{v}_i$ as translational velocity of the output link. Among $\hat{\mathbf{S}}_{TWS,i}$, all except $\hat{\mathbf{S}}_{TWS,k}$ are constraint wrenches applying no work to the output link [\[42\]](#). Thus, the unknown motions at the connecting joints can be derived by the reciprocal condition

$$\delta W_i = \hat{\mathbf{S}}_{TWS,i} \circ {}^{(k)}\mathbf{S}_{OTS} = 0 \quad (20)$$

where the underdeterminedness is resolved by an additional equation, for instance, setting the sum of all entries of ${}^{(k)}\mathbf{S}_{OTS}$ to 1. Note that the system may not be defined fixing a single entry only. Serving as example, it follows if the first chain is removed

$$\left| \begin{array}{l} \hat{f}_2^{(k)} \mathbf{v}_1 = 0 \\ \hat{f}_3^{(k)} \mathbf{v}_1 = 0 \end{array} \right| \rightarrow \mathbf{S}_{OTS,1} = \begin{bmatrix} \mathbf{0}_3 \\ \mathbf{v}_1 \end{bmatrix} = \begin{bmatrix} \mathbf{0}_3 \\ \hat{f}_3 \times \hat{f}_2 / \| \hat{f}_3 \times \hat{f}_2 \| \end{bmatrix} \quad (21)$$

For the output transmission index, the resulting unit output twist screws (OTS) are related to the corresponding TWS. As illustrated by the virtual joint $X_{OTI,k}$ in [Fig. 3\(a\)](#), it is presumed that the output link performs translational motion only (which disregards potential constraint singularities). Accordingly, the angular velocity of the OTS is zero. Then, for infinite pitch screws (pure translation), the maximum virtual coefficient is simply given by the maximum value of the dot product of the wrench and twist axes, which is one in this case [\[36\]](#). Then, the related power coefficient taking into account three supporting links only is

$$\eta_1 = |\mathbf{S}_{TWS,1} \circ \mathbf{S}_{OTS,1}| = \left| \hat{f}_1^T (\hat{f}_3 \times \hat{f}_2) \right| / \left\| \hat{f}_3 \times \hat{f}_2 \right\| \quad (22)$$

which, since the maximum virtual coefficient is one, corresponds to the orthogonal product of wrench and twist screws. The same applies for the second and third chain, which finally gives the output transmission index based on three supporting

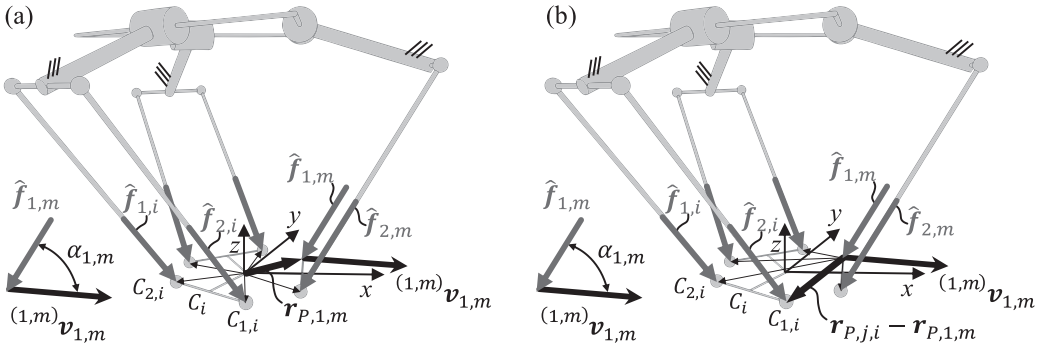


Fig. 4. Geometric relations: output transmission index with six supporting links.

links

$$OTI_3 = \min(\eta_1, \eta_2, \eta_3) \quad (23)$$

Similar approaches can be found for fully parallel 4-dof Delta variants with four overconstrained kinematic chains, cf. [63,64].

3.4.2. Three supporting links (Including constraint characteristics)

Delta-related analyses of the output transmission based on power coefficients without consideration of the constrainability can, for example, be found for the non-overconstrained 3-R(2-SS) Delta robot [65]. The approach is however not generally valid since it cannot be guaranteed that the output link is sufficiently constrained for any configuration. Following the constraint analyses, e.g., presented in [9–11], the constraint moments of the 3-R(2-SS) can be derived. Accordingly, the rotational dof of the platform are restraint by three couples orthogonal to each of the parallelograms, i.e.,

$$\mathbf{S}_i^r = \begin{bmatrix} \mathbf{0}_3 \\ \hat{\mathbf{e}}_i \times \hat{\mathbf{f}}_i \end{bmatrix} = \begin{bmatrix} \mathbf{0}_3 \\ \mathbf{n}_i \end{bmatrix} \quad (24)$$

In contrast to the overconstrained variant 3-R(RPaR), the three constraint moments \mathbf{n}_i of the industrial variant 3-R(2-SS) may become linearly dependent for specific positions of the platform (e.g., configurations, in which all connecting rods are parallel).

Hence, the constraint capabilities must be assessed, for instance, by additionally taking into account the constraint wrench system. Following the approach presented in [57], a single-dof virtual motion of the robot is generated restraining the output link by a 5-system of the three actuation wrench screws and two of the three constraint wrench screws (CWS) known from (24), cf. Fig. 3(b). Then, a virtual joint $\chi_{CTI,k}$ allows the platform to perform a 1-dof motion given by the restricted twist screw (RTS), which is found by

$$\delta W_i = \mathbf{S}_{WS,i} \circ {}^k\mathbf{S}_{RTS} = 0 \quad \forall i \neq k \quad (25)$$

and finally establishes the related power coefficient

$$\varepsilon_i = \frac{|\mathbf{S}_{CWS,i} \circ {}^i\mathbf{S}_{RTS}|}{|\mathbf{S}_{CWS,i} \circ {}^i\mathbf{S}_{RTS}|_{\max}} \quad (26)$$

The constraint transmission index is derived by

$$CTI = \min(\varepsilon_1, \varepsilon_2, \varepsilon_3) \quad (27)$$

The output transmission index OTI_3 and the constraint transmission index CTI may be sufficient to assess the transmissibility and constrainability of a parallel robot, which is critically questioned in the following.

3.4.3. Six supporting links (general approach)

Since OTI_3 measures the transmissibility (i.e., the quality of force transmission from the output to the input) and CTI measures the constrainability (i.e., the closeness to a constraint singularity), the two indices should not be aggregated to a single index. But a single index may be beneficial for design optimization purposes.

For parallel robots, in which the output link is supported by six links, from which thus each is connected to the output link by spherical joints, it is however not necessary to evaluate separately the constraint indices. In these special cases, the transmission wrench screws (TWS) at the application points (i.e., spherical joints) degenerate to transmission force lines. The TWS of rod (j, i) with respect to a platform-related spherical joint $C_{j,i}$ (Fig. 4(a)) are then given by

$$\hat{\mathbf{S}}_{TWS,j,i} = \begin{bmatrix} \hat{\mathbf{f}}_{j,i} \\ \mathbf{r}_{P,j,i} \times \hat{\mathbf{f}}_{j,i} \end{bmatrix} \quad (28)$$

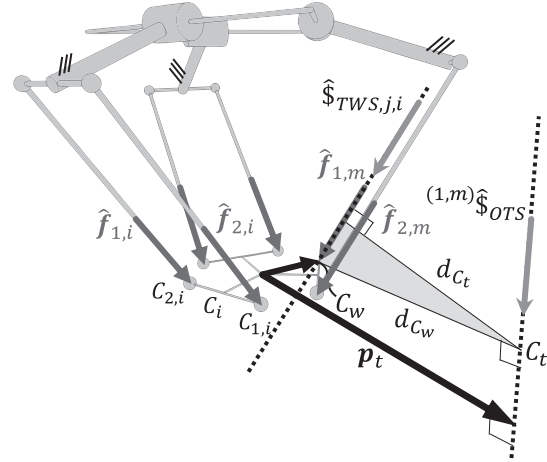


Fig. 5. Relations simplifying the general definition of the power coefficient.

with $\mathbf{r}_{P,j,i}$ as vector from the origin of the platform to the respective joint. Imagine the virtual motion of a single-dof mechanism by fixing all three input and removing one of the six connecting rods k of a chain m (Fig. 4(a), $k = 1$) [37]. The instantaneous motion of the output link is then given by

$${}^{(k,m)}\hat{\mathbf{s}}_{OTS} = \begin{bmatrix} {}^{(k,m)}\boldsymbol{\omega} \\ {}^{(k,m)}\mathbf{v}_{j,i} \end{bmatrix} \quad (29)$$

with ${}^{(k,m)}\boldsymbol{\omega}$ as angular velocity and ${}^{(k,m)}\mathbf{v}_{j,i}$ as translational velocity at joint $C_{j,i}$ of the output link. Among $\hat{\mathbf{s}}_{TWS,j,i}$, all except $\hat{\mathbf{s}}_{TWS,k,m}$ are constraint wrenches and thus it follows

$$W_{j,i} = \hat{\mathbf{s}}_{TWS,j,i} \circ {}^{(k,m)}\hat{\mathbf{s}}_{OTS} = \hat{\mathbf{s}}_{TWS,j,i} \circ \begin{bmatrix} {}^{(k,m)}\boldsymbol{\omega} \\ {}^{(k,m)}\mathbf{v}_{j,i} \end{bmatrix} = 0 \quad (30)$$

where $\forall i \neq m$ and $\forall j \neq k$. Finally, the power coefficient taking into account six supporting links following the general approach is

$$\rho_{k,m} = \frac{|\hat{\mathbf{s}}_{TWS,k,m} \circ {}^{(k,m)}\hat{\mathbf{s}}_{OTS}|}{|\hat{\mathbf{s}}_{TWS,k,m} \circ {}^{(k,m)}\hat{\mathbf{s}}_{OTS}|_{max}} \quad (31)$$

3.4.4. Six supporting links (simplified approach)

The pose-dependent maximum virtual coefficient can be simplified for the Delta robot. Following the general procedure in [58] and the notion introduced in Section 3.2, the distance between the TWS and OTS is either measured perpendicular to the TWS axis or to the OTS axis. However, in case of spherical connecting joints (resulting in pure forces) the maximum distance is always given as orthogonal distance on the twist screw axis (Fig. 5). A pure force in turn is represented by a transmission force line, which is a zero-pitch screw. Thus, the computation of the maximum virtual coefficient is simplified as follows

$$|\hat{\mathbf{s}}_{TWS,k,m} \circ {}^{(k,m)}\hat{\mathbf{s}}_{OTS}|_{max} = \sqrt{(h_{TWS} + h_{OTS})^2 + d_{max}^2} = \sqrt{h_{OTS}^2 + d_{C_w}^2} \quad (32)$$

An example of such simplification for a 6-PUS can be found in [66]. This approach however can be further simplified by defining the TWS at the six spherical joints (Fig. 4(b)), i.e.,

$$\hat{\mathbf{s}}_{TWS,j,i} = \left[(\mathbf{r}_{P,j,i} - \mathbf{r}_{P,k,m}) \times \hat{\mathbf{f}}_{j,i} \right] \quad (33)$$

In this case, the tedious computation of the maximum virtual coefficient is not required at all since the TWS is given as a pure force and without a couple. Solving the five reciprocal conditions analogously to the previous approaches gives the unknown OTS at the unfixed connecting rod.

The virtual coefficient is thus given by the dot product of the pure force and the linear velocity at the respective connecting joint. This also means that the maximum virtual coefficient is one. Thus, the power coefficient is the cosine of the

Table 2
Design parameter values.

Parameter	$r_{E,i}$ [m]	$r_{P,i}$ [m]	$l_{PL,i}$ [m]	$l_{DL,i}$ [m]	D_S [m]
Value	0.20	0.05	0.40	0.80	0.10

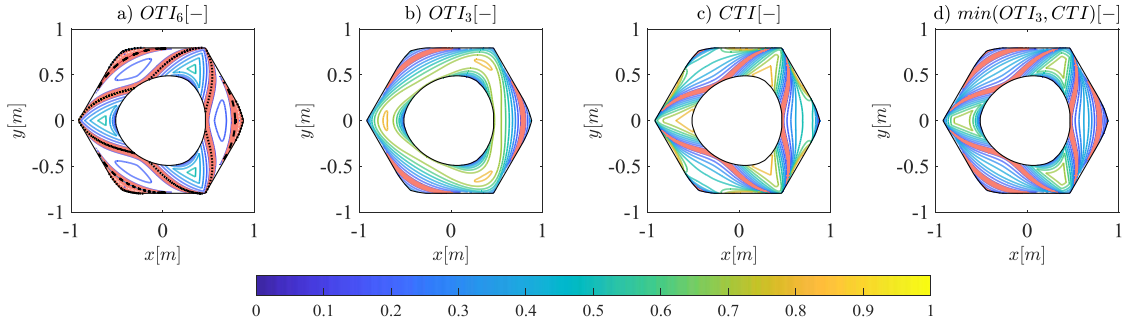


Fig. 6. Distributions following alternative definitions of the output and constraint transmission indices (with singular regions marked in red). (For interpretation of the references to color in this figure legend, the reader is referred to the web version of this article.)

pressure angles at the six connecting joints at the output link, i.e.,

$$\eta_{k,m} = \cos(\alpha_{k,m}) = \frac{(k,m)\mathbf{v}_{k,m}^T \hat{\mathbf{f}}_{k,m}}{\| (k,m)\mathbf{v}_{k,m} \|} \quad (34)$$

The related output transmission index based on six supporting links then is

$$OTI_6 = \min(|\eta_{k,m}|) \quad \forall m = \{1, 2, 3\}, \quad \forall k = \{1, 2\} \quad (35)$$

4. Suitability assessment for practical application

The following section proves that the newly defined index OTI_6 using six supporting links can be used to analyze the global wrench system and at the same time successfully detects all types of singularities of the Delta parallel robot. Furthermore, the effectiveness of using the proposed indices for kinematic performance optimization is emphasized.

4.1. Application to kinematic performance evaluation

Based on Sect. 3, the input transmission characteristics are unequivocal, whereas four distinct approaches for the evaluation of output transmission characteristics were derived, from which the general and simplified approaches with six supporting links lead to the same results. Based on the design parameter values as summarized in Table 2, Fig. 6(a) and (b) shows two different distributions of the OTI measured for a critical horizontal layer ($Z = -0.24$ m) within the reachable workspace. It should be noted that for practical applications, such configurations are unlikely to occur due to restrictions of the joint motion angles or otherwise self-collision.

Regions where OTI become less than 0.1 are highlighted in red. Here, based on the relationship between the output pose error and the transmission index (TI) for the 6-SPS mechanism in [67], the threshold value to identify the neighborhoods of singularity is set to 0.1. Note that an exact threshold value to distinguish between singular and non-singular configurations does not exist.

Fig. 6(a) clearly demonstrates that OTI successfully detects neighborhoods, where actuation (dashed line) or constraint (dotted line) singularities occur. Presuming translational (virtual) motion of the output link with three supporting links, the related OTI_3 fails to detect the internal (constraint) singularities. However, minimal values ($OTI_3 \leq 0.1$) correspond to singular point-curves of actuation (Fig. 6(b)).

For thorough analyses, separate investigations of the constraint transmission index CTI are unavoidable. Then, constraint singularities are successfully detected (Fig. 6(c)). Nonetheless, the definitions of OTI_3 and CTI are based on virtual situations, which are not physically appropriate. For instance, for the CTI , the relation between the constraint wrench moment and the (virtual) rotational motion of the output link is evaluated. In practice, such situation does not exist. Moreover, difficulties may arise for the determination of a unique index, which may be the minimum or the product of OTI_3 and CTI including weightings. As an example, Fig. 6(d) shows the distribution of the minimum of OTI_3 and CTI (without weightings). Obviously, the combination successfully detects all singular configurations, actual values however have no physical meaning and thus, are different from the distribution following the physically appropriate concept with six supporting links, i.e., OTI_6 . Accordingly, deviations fluctuate up to +0.37 (subtracting OTI_6 from the combined indices OTI_3 and CTI , cf. Fig. 7(a)).

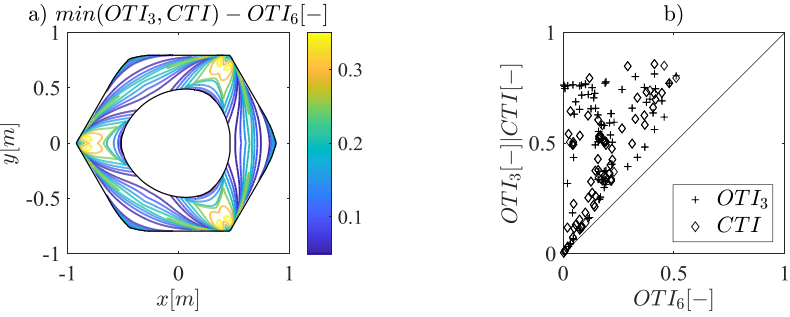


Fig. 7. Relations between output and constraint transmission indices.

In addition, Fig. 7(b) separately displays OTI_3 and CTI over OTI_6 . Similarly, it can be seen that both OTI_3 and CTI overestimate the physically appropriate index OTI_6 . This overestimation slightly increases with increasing OTI_6 . In other words, OTI_6 is a lower bound for OTI_3 and CTI . More importantly, the closeness to both, actuation and constraint singularity, is underestimated. Note that this underestimation can also be observed comparing the regions denoting near-singular configurations based on the predetermined threshold value in Fig. 6. Accordingly, smaller critical regions are observed for OTI_3 and CTI . In conclusion, OTI_6 successfully aggregates two separate indices for force transmissibility and constrainability into a single performance index, which is beneficial for the application in kinematic design optimization task as discussed in the following section.

4.2. Application to kinematic performance optimization

Design optimization of robotic systems usually involves multiple conflicting objectives (such as optimizing the velocity and force transmission based on the kinematic Jacobian matrix). Accordingly, the optimal solution for the related multi-objective optimization approach is not given as a single optimum but as trade-off or compromise between multiple objectives. Multiple objectives may be condensed into a single objective, e.g., by the product or linear combination of the objectives using weighting factors. Nevertheless, it seems more convenient to know the potential trade-off solutions and then decide based on further evaluation and selection criteria.

Deterministic approaches, e.g., gradient-based methods, work well for single-objective optimizations. However, they may converge to local optima depending on the problem complexity and the selected start solutions. To escape from local optima and potentially find globally optimal solutions to multiple-objective optimizations, stochastic approaches, e.g., evolutionary algorithms and even random approaches, can be employed. Evolutionary algorithms are inspired by the nature's evolutionary principle [68]. In simple words, each iteration involves candidates (population), which are evaluated and systematically further developed in subsequent generations. Finally, multiple non-dominated solutions, so-called Pareto-optimal candidates, can be found.

In this context, ITI and OTI_6 may be evaluated for a discrete set of evaluation points within the reachable or prescribed workspace. Then the performance for the entire set is taken into account as objective for the design optimization. Commonly, the overall performance is based on the minimum, mean and/or standard deviation of the respective index over the set of evaluation points, cf. e.g., [69,70]. Here, the minima ITI_{min} and OTI_{min} are taken into account.

For industrially relevant workspace requirements, the objectives ITI_{min} and OTI_{min} show antagonistic behavior resulting in hyperbolic Pareto fronts. High values for ITI_{min} lead to low values for OTI_{min} . In addition, preliminary analyses in [6] reveal a relation between optimal kinematic characteristics and the envelope ratio ϑ , i.e., the ratio of workspace to robot envelope. Accordingly, the Pareto front is shifted toward better results for both criteria ITI_{min} and OTI_{min} when ϑ is reduced (i.e., when the requirements on the envelope ratio is less demanding) and vice versa.

Instead of considering OTI_{min} as a separate optimization criterion, it is commonly proposed to combine the transmission indices taking into account the minimum or the product of ITI_{min} and OTI_{min} . If OTI_{min} is smaller than ITI_{min} (which is likely for industrially relevant design candidates), a consideration of minimal values ensures a singular-free design but fails to improve ITI_{min} . Moreover, in combination with dynamic objectives both of the latter approaches (minimum and product) would lead to rather small values for ITI_{min} as OTI_{min} is preferably increased to simultaneously allow for smaller torques (but also smaller ITI_{min}). The reason for this is the positive correlation of ITI_{min} with the actuation speed, which in turn is (by tendency) negatively correlated with the dynamics characteristics and the actuation torque, respectively. It should also be noted that OTI_{min} can be directly influenced by the distance between the spherical joints D_S (cf. Fig. 1 and (33)) and thus without affecting ITI_{min} . This feature can eventually be used to compensate potential losses in OTI_{min} in order to allow for higher ITI_{min} . Moreover, following the proposed definition of the output transmission characteristics, the distances between the spherical joints can be used D_S as additional design parameter, which is novel. Besides this a limited pressure angle of the input transmission can be used as design constraint [6], where the $\gamma_i \leq 50^\circ$ is suggested for practical application [71].

The effectiveness of the proposed indices for kinematic performance optimization shall be demonstrated in the following case study. Accordingly, ITI_{min} and OTI_{min} are employed to find kinematically superior designs for four different industrially

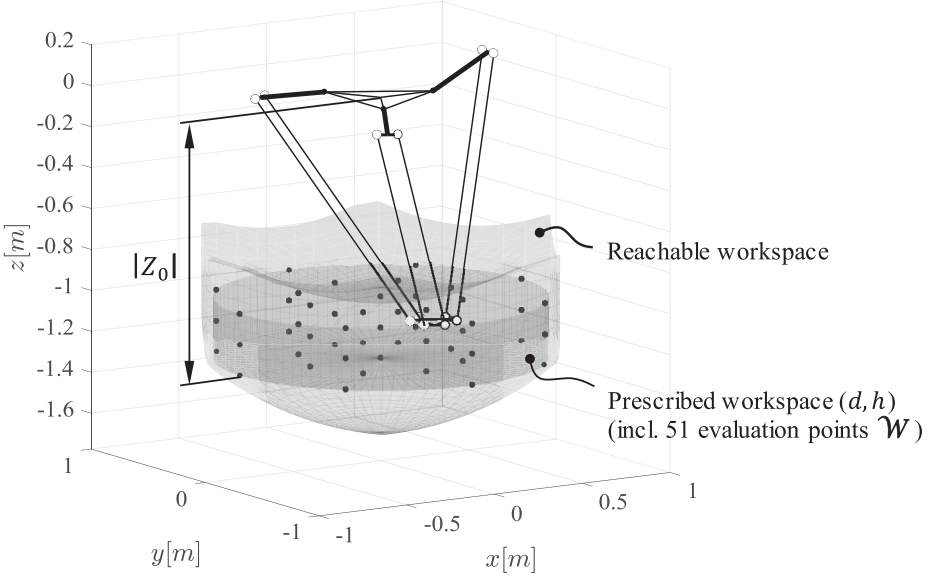


Fig. 8. Definition of the prescribed workspace.

Table 3
Comparison of optimized candidates (OPT) with industrial benchmarks (IBM).

Variant	d [m]	h [m]	$r_{F,i}$ [m]	$r_{P,i}$ [m]	$l_{PL,i}$ [m]	$l_{DL,i}$ [m]	D_S [m]	$ Z_0 $ [m]	ITI_{min} [-]	OTI_{min} [-]	ϑ [-]
IBM I	0.800	0.200	0.200	0.045	0.235	0.800	0.100	0.828	0.608	0.351	0.294
OPT I	0.800	0.200	0.205	0.045	0.449	0.637	0.100	0.788	0.683	0.354	0.281
IBM II	1.200	0.200	0.250	0.067	0.375	0.960	0.100	0.935	0.709	0.299	0.261
OPT II	1.200	0.200	0.202	0.067	0.324	1.216	0.130	1.228	0.763	0.300	0.260
IBM III	1.600	0.300	0.200	0.045	0.432	1.106	0.100	1.063	0.540	0.232	0.416
OPT III	1.600	0.300	0.200	0.045	0.396	1.253	0.100	1.241	0.566	0.233	0.411
IBM IV	2.000	0.500	0.333	0.140	0.700	1.650	0.182	1.737	0.701	0.250	0.350
OPT IV	2.000	0.500	0.222	0.140	0.798	1.698	0.182	1.820	0.753	0.264	0.350

relevant workspace sizes. The solutions are then compared to related industrial benchmarks (IBM I-IV), where the workspace parameters and kinematic properties are inspired by the commercial variants ABB IRB 360-1/800 FlexPicker (IBM I), MAJA-tronic/Autonox 24 RL3-1200 (IBM II), ABB IRB 360-1/1600 FlexPicker (IBM III), and MAJAtronic/Autonox 24 RL3-2000 (IBM IV). Their prescribed workspaces are composed of a cylinder with either a conical or an ellipsoidal portion adjacent to it. The center of their connecting surface determines the relative position $P_0 = [0, 0, Z_0]$ of the workspace to the origin of frame, where $|Z_0|$ is used as design variable (cf. Fig. 8). Here only the related cylinder with diameter d and height h is considered, cf. Table 3 and Fig. 8. The kinematic performance of the solution candidates are then assessed based on 51 evaluation points \mathcal{W} on three characteristic layers within the prescribed workspace (i.e., bottom, middle, top). The number of points is given by a distribution on two radii in 45° steps plus the central axis, i.e., $3 \cdot 2 \cdot 8 + 3 = 51$ coordinates, cf. Fig. 8.

Presuming a symmetric architecture, five parameters are predestined for optimization, i.e.,

$$\mathcal{P} = [r_F, r_P, l_{PL}, l_{DL}, |Z_0|]. \quad (36)$$

As objective function to be maximized, the minimal values of the input and output transmission indices (ITI_{min} and OTI_{min}) as well as the workspace to robot envelope ratio ϑ are taken into account, which gives

$$\text{maximize } z = (\mathbf{f}_1(\mathcal{P}, \mathcal{W}), \mathbf{f}_2(\mathcal{P}, \mathcal{W}), \mathbf{f}_3(\mathcal{P}, \mathcal{W}) = (ITI_{min}, OTI_{min}, \vartheta)) \quad (37)$$

$$\text{subject to } \mathbf{g}(\mathcal{P}, \mathcal{W}) \quad (38)$$

where \mathbf{g} denotes the set of constraints as derived from the requirements.

The requirements arise from parametric relations based on practical implementation (i.e., the maximum joint motion angle of the spherical joints and the minimum distance between two adjacent spherical joints), kinematic characteristics (i.e., the reachability of all positions within the prescribed workspace while avoiding dead center positions and complying with maximum allowable pressure angles), or experience-based conditions such as maximum link length ratio. For the sake of brevity, the detailed derivation is not shown here. The optimization problem is solved using the Nondominated Sorting Genetic Algorithm II (NSGA-II) in Matlab, which is successfully applied to other parallel robots in [64,72–74]. For detailed descriptions of the fundamental principle of the NSGA-II, it is referred to [68]. Due to undetermined or ambiguous

definitions of the relative distance to the base frame, the IBM are first optimized for ITI_{min} and OTI_{min} . Here, solely the unknown relative distance to the base frame $|Z_0|$ is used as decision variable, while all other parameters are given and thus remain unaffected.

As a simplification, the candidate with the best input characteristics is selected from the set of Pareto optimal solutions. This can be justified by the strong correlation of ITI_{min} with the power efficiency in light-weight high-speed robots. For the actual optimization task, r_F , l_{PL} , l_{DL} , and $|Z_0|$ are used as decision variables, whereas the platform radii r_p and distances between the spherical joints D_S are assumed to correspond to the respective benchmark robot. Table 3 summarizes the optimization results (OPT I-IV) in comparison with the industrial benchmarks.

It can be seen that each IBM is dominated by the respective optimal result (OPT) in both objectives, while similar requirements on the envelope ratio ϑ are met. Note that the solutions can be further improved by relaxation of the constraints and/or allowing a lower ϑ . As an exception, the distances between the spherical joints D_S of OPT II needed to be increased subsequently in order to improve OTI_{min} and eventually obtain a superior result. It should be mentioned, that (a) the shapes and sizes of the prescribed workspaces of the IBM differ from the prescribed workspaces in this study (only the cylinder portions were taken into account), (b) the definitions of relative positions of the workspace layer were approximated, and (c) the underlying constraints (potentially including dynamic characteristics) as used for the design of the IBM are unknown and may restrict the design parameter in a different way.

5. Conclusions

As kinematic evaluation indices, the input transmission index and the output transmission index were derived following previous approaches based on the notion of virtual power coefficients and pressure angles. The newly derived output transmission index OTI_6 aggregates the conventional indices OTI_3 and CTI into a single, physically appropriate index, while successfully detecting all singularities and accurately evaluating the motion/force transmissibility and constrainability for Delta Parallel Robots, one of the best-known lower-dof parallel robot. Furthermore, due to the simple definition related to the points of application (i.e., the spherical joints), the output transmission index OTI_6 refers to the pressure angles of the output transmission. Associated therewith, the tedious computation of the normalization factor can be avoided. The evaluation results obtained by OTI_6 agrees with the results obtained by the conventional approach based on the separate indices OTI_3 and CTI , which proves the validity of the new approach. A suitability assessment for application highlighted the special characteristics of the different indices and their interactions in the application fields of performance evaluation and optimization.

References

- [1] V.E. Gough, Contribution to discussion of papers on research in automobile stability, control and tyre performance, Proc. Inst. Mech. Eng. Autom. Div. (1956) 392–394.
- [2] D. Stewart, A platform with six degrees of freedom, Proc. Inst. Mech. Eng. 180 (1) (1965) 371–386.
- [3] J. Brinker, B. Corves, A survey on parallel robots with Delta-like architecture, in: *Proc. of the 14th IFToMM World Congress in Mechanism and Machine Science*, Taipei, 2015.
- [4] S. Riazi, O. Wigström, K. Bengtsson, B. Lennartson, Energy and peak power optimization of time-bounded robot trajectories, IEEE Trans. Autom. Sci. Eng. 14 (2) (2017) 646–657 April.
- [5] B.L. Capeci, W.C. Turner, W.J. Kennedy, Guide to Energy Management, 8th Edition, International Version, CRC Press, 2016.
- [6] J. Brinker, B. Corves, Y. Takeda, Kinematic and dynamic dimensional synthesis of extended Delta parallel robots, in: *Proc. of the 5th IFToMM International Symposium on Robotics & Mechatronics (ISR&M 2017)*, Sydney, Australia, 2017 29 November–1 December.
- [7] J.K. Davidson, K.H. Hunt, *Robots and Screw Theory: Applications of Kinematics and Statics to Robotics*, Oxford University Press, 2004.
- [8] X.-J. Liu, C. Wu, J. Wang, A new approach for singularity analysis and closeness measurement to singularities of parallel manipulators, J. Mech. Robot. 4 (4) (2012).
- [9] J. Yu, J.S. Dai, T.S. Zhao, S. Bi, G. Zong, Mobility analysis of complex joints by means of screw theory, Robotica 27 (6) (2009) 915–927.
- [10] T. Zhao, J.S. Dai, Z. Huang, Geometric analysis of overconstrained parallel manipulators with three and four degrees of freedom, JSME Int. J. Series C 45 (3) (2002).
- [11] S. Amine, D. Kanaan, S. Caro, P. Wenger, Constraint and singularity analysis of lower-mobility parallel manipulators with parallelogram joints, in: *Proc. of the ASME IDETC/CIE 2010*, Montreal, 15–18, Quebec, Canada, 2010 August.
- [12] Y.J. Lou, G.F. Liu, Z.X. Li, A general approach for optimal design of parallel manipulators, in: *Proc. of the ICRA 2004*, New Orleans, LA, USA, 2004 26 April–1 May.
- [13] A. de-Juan, J.-F. Collard, P. Fisette, P. Garcia, R. Sancivrian, Multi-objective optimization of parallel manipulators, New Trends Mech. Sci. (2010).
- [14] J. Angeles, *Fundamentals of Robotic Mechanical Systems*, Springer, 2014.
- [15] J.K. Salisbury, J.J. Craig, Articulated hands: force control and kinematic issues, Int. J. Robot. Res. 1 (1) (1982).
- [16] C.M. Gosselin, J. Angeles, The optimum kinematic design of a planar three-degree-of-freedom parallel manipulator, J. Mech. Trans. Autom. Des. 110 (1) (1988).
- [17] B. Siciliano, O. Khatib (Eds.), *Springer Handbook of Robotics*, 2016.
- [18] T. Yoshikawa, Manipulability of robotic mechanisms, Int. J. Robot. Res. 4 (2) (1985).
- [19] J.-O. Kim, P.K. Khosla, Dexterity measures for design and control of manipulators, in: *Proc. of the IROS 1991*, 3–5 November, Osaka, Japan, 1991.
- [20] J. Angeles, On the optimum dimensioning of robotic manipulators, in: *Department of Mechanical Engineering & Centre for Intelligent Machine*, McGill University, Montreal, 2004, p. 14. pages.
- [21] P. Cardou, S. Bouchard, C.M. Gosselin, Kinematic-sensitivity indices for dimensionally nonhomogeneous Jacobian matrices, IEEE Trans. Robot. 26 (1) (2010).
- [22] C.A. Klein, B.E. Blaho, Dexterity measures for the design and control of kinematically redundant manipulators, Int. J. Robot. Res. 6 (2) (1987) 72–83.
- [23] J.-P. Merlet, *Parallel Robots*, 2nd Edition, Springer, 2006.
- [24] W.A. Khan, J. Angeles, The kinetostatic optimization of robotic manipulators: the inverse and the direct problems, ASME J. Mech. Des. 128 (2006) January.

- [25] J. Kim, C. Park, J. Kim, F.C. Park, Performance analysis of parallel mechanism architectures for CNC machining applications, *J. Manuf. Sci. Eng.* 122 (2000) 753–759 November.
- [26] S.A. Joshi, L.-W. Tsai, Jacobian analysis of limited-DOF parallel manipulators, *J. Mech. Des.* 124 (2) (2002) 254–258.
- [27] F. Xie, X.-J. Liu, J. Li, Performance indices for parallel robots considering motion/force transmissibility, in: X. Zhang, H. Liu, Z. Chen, N. Wang (Eds.), *Intelligent Robotics and Applications. ICIRA 2014. Lecture Notes in Computer Science*, Springer, Cham, 2014 8917.
- [28] Y. Lou, D. Zhang, Z. Li, Optimal design of a parallel machine based on multiple criteria, in: *Proc. of the ICRA 2005*, Barcelona, Spain, 2005, pp. 18–22. April.
- [29] R. Kelaiaia, O. Company, A. Zaatri, Multiobjective optimization of a linear Delta parallel robot, *Mech. Mach. T.* 50 (2012) 159–178.
- [30] C. Chen, *The Design of Innovative Epicyclic Mechanical Transmissions Application to the Drives of Wheeled Mobile Robots*, Department of Mechanical Engineering, McGill University, Montréal, 2006.
- [31] H. Alt, Der Übertragungswinkel und seine Bedeutung für das Konstruieren periodischer Getriebe, *Werkstattechnik* 26 (1932) 61–64.
- [32] M.S.C. Yuan, F. Freudenstein, L.S. Woo, Kinematic analysis of spatial mechanism by means of screw coordinates. part 2 – analysis of spatial mechanisms, *J. Eng. Ind.* 91 (1) (1971) 67–73.
- [33] R.S. Ball, *A Treatise on the Theory of Screws*, 1900.
- [34] G. Sutherland, B. Roth, A transmission index for spatial mechanisms, *J. Eng. Ind.* 95 (2) (1973) 589–597.
- [35] M.J. Tsai, H.W. Lee, The transmissivity and manipulability of spatial mechanisms, *J. Mech. Des.* 116 (1994) 137–143.
- [36] C. Chen, J. Angeles, Generalized transmission index and transmission quality for spatial linkages, *Mech. Mach. T.* 42 (2007) 1225–1237.
- [37] Y. Takeda, H. Funabashi, Motion transmissibility of in-parallel actuated manipulators, *JSME Int. J. Series C* 38 (4) (1995) 749–755.
- [38] Y. Takeda, H. Funabashi, A transmission index for in-parallel wire-driven mechanisms, *JSME Int. J. Series C* 44 (1) (2001) 180–187.
- [39] Y. Takeda, H. Funabashi, Y. Sasaki, Development of a spherical in-parallel actuated mechanism with three dof with large working space and high motion transmissibility, *JSME Int. J. Series C* 39 (3) (1996) 541–548.
- [40] S. Briot, V. Galzunov, V. Arakelian, Investigation of the effort transmission in planar parallel manipulators, *J. Mech. Robot.* 7 (2013).
- [41] H. Shimojima, K. Ogawa, T. Kawano, A Transmissibility for single-loop spatial mechanism, *Bull. JSME* 22 (165) (1997) 405–411.
- [42] J. Wang, C. Wu, X.-J. Liu, Performance evaluation of parallel manipulators: motion/force transmissibility and its index, *Mech. Mach. T.* 45 (2010) 1462–1476.
- [43] F. Xie, X.-J. Liu, J. Wang, Performance evaluation of redundant parallel manipulators assimilating motion/force transmissibility, *Int. J. Adv. Robot. Syst.* 8 (5) (2011) 113–124.
- [44] H. Liu, T. Huang, A. Kecskeméthy, D.G. Chetwynd, Force/motion/stiffness transmissibility analyses of redundantly actuated and overconstrained parallel manipulators, in: *Proc. of the 14th IFTOMM World Congress in Mechanism and Machine Science*, Taipei, 2015 Oct.
- [45] L.-W. Tsai, *Robot Analysis: The Mechanics of Serial and Parallel Manipulators*, Wiley, 1999.
- [46] X.-J. Liu, J. Wang, *Parallel Kinematics – Type, Kinematics, and Optimal Design*, Springer, 2014.
- [47] D. Zlatanov, R.G. Fenton, B. Benhabib, Identification and classification of the singular configurations of mechanisms, *Mech. Mach. Theory* 33 (6) (1998) 743–760 August.
- [48] G. Gogu, *Structural Synthesis of Parallel Robots – Part 1: Methodology*, Springer, 2009.
- [49] S. Amine, L. Nurahmi, P. Wenger, S. Caro, *Conceptual Design of Schoenflies Motion Generators Based on the Wrench Graph*, ASME IDETC/CIE, USA, 2013 Aug.
- [50] D. Kanaan, P. Wenger, S. Caro, D. Chablat, Singularity analysis of lower-mobility parallel manipulators using Grassmann–Cayley algebra, *IEEE Trans. Robot.* 25 (5) (2009) 995–1004 October.
- [51] S. Amine, M. Tale-Masouleh, S. Caro, P. Wenger, C.M. Gosselin, Singularity analysis of the 4-RRU parallel manipulator using Grassmann–Cayley algebra, *ASME IDETC/CIE 2014, Volume 6: 35th Mechanisms and Robotics Conference, Parts A and B*, 2011 August 28–31.
- [52] D. Zlatanov, I.A. Bonev, C.M. Gosselin, Constraint singularities of parallel mechanisms, in: *Proc. of the ICRA 2002*, Washington DC, USA, 2002 May.
- [53] S. Amine, M. Tale-Masouleh, S. Caro, P. Wenger, C.M. Gosselin, Singularity conditions of 3T1R parallel manipulators with identical limb structures, *J. Mech. Robot.* 4 (1) (2012) 11 pages.
- [54] X.-J. Liu, C. Wu, J. Wang, A new approach for singularity analysis and closeness measurement to singularities of parallel manipulators, *J. Mech. Robot.* 4 (4) (2012).
- [55] C. Wu, X.-J. Liu, F. Xie, J. Wang, New measure for ‘closeness’ to singularities of parallel robots, in: *Proc. of the ICRA 2011*, Shanghai, 2011.
- [56] X.-J. Liu, X. Chen, M. Nahon, Motion/force constrainability analysis of lower-mobility parallel manipulators, *J. Mech. Robot.* 6 (2014).
- [57] X. Chen, X.-J. Liu, F. Xie, Screw theory based singularity analysis of lower-mobility parallel robots considering the motion/force transmissibility and constrainability, *Math. Prob. Eng.* 3 (2015).
- [58] H. Liu, T. Huang, A. Kecskeméthy, D. Chetwynd, A generalized approach for computing the transmission index of parallel mechanisms, *Mech. Mach. T.* 74 (2014) 245–256.
- [59] J. Brinker, B. Corves, Y. Takeda, On the motion/force transmissibility and constrainability of Delta parallel robots, in: *Proc. of 7th IFTOMM Inter. Workshop on Computational Kinematics (CK2017)*, 22–24, Futuroscope-Poitiers, France, 2017 May.
- [60] Y. Takeda, X. Liang, Transmission index of lower-mobility parallel mechanism – case study on 3-PRS mechanism, in: *Proc. of the ASME IDETC/CIE 2017*, Cleveland, USA, 2017 Aug.
- [61] L. Nurahmi, *Kinematic Analysis and Design of Parallel Manipulators with Multiple Operation Modes*, École Centrale de Nantes, 2015.
- [62] J. Zhao, Z. Feng, F. Chu, N. Ma, *Advanced Theory of Constraint and Motion Analysis For Robot Mechanisms*, Academic Press, 2013.
- [63] F. Xie, X.-J. Liu, Design and development of a high-speed and high-rotation robot with four identical arms and a single platform, *J. Mech. Robot.* 7 (2015).
- [64] G. Wu, S. Bai, P. Hjørnet, Multi-objective design optimization of a parallel schönhflies-motion robot, *Adv. Rec. Mech. Rob.* II (2016) 657–667.
- [65] L. Zhang, J. Mei, X. Zhao, T. Huang, Dimensional synthesis of the Delta robot using transmission angle constraints, *Robotica* 30 (2011) 343–349.
- [66] Y. Takeda, H. Funabashi, H. Ichimaru, Development of spatial in-parallel actuated manipulators with six degrees of freedom with high motion transmission, *JSME Int. J. Ser. C* 40 (2) (1997) 299–308.
- [67] Y. Takeda, H. Funabashi, Kinematic and static characteristics of in-parallel actuated manipulators at singular points and in their neighborhood, *JSME Int. J. Ser. C* 39 (1) (1996) 85–93.
- [68] K. Deb, in: *Multi-Objective Optimization Using Evolutionary Algorithms*, John Wiley & Sons, Chichester, 2001, p. 515.
- [69] C. Wu, X.-J. Liu, L. Wang, J. Wang, Optimal design of spherical 5r parallel manipulators considering the motion/force transmissibility, *J. Mech. Des.* 132 (3) (2010).
- [70] T. Huang, M. Wang, S. Yang, T. Sun, D.G. Chetwynd, F. Xie, Force/motion transmissibility analysis of six degree of freedom parallel mechanisms, *J. Mech. Robot.* 6 (2014) August.
- [71] T. Huang, Z. Li, M. Li, D.G. Chetwynd, C.M. Gosselin, Conceptual design and dimensional synthesis of a novel 2-DOF translational parallel robot for pick-and-place operations, *J. Mech. Des.* 126 (2004) 449–455 May.
- [72] C. Germain, S. Briot, S. Caro, J.B. Izard, C. Baradat, Task-oriented design of a high-speed parallel robot for pick-and-place operations, in: *Proc. of the ICRA 2014 (WS)*, Hong Kong, China, 2014 31 May – 5 June.
- [73] G. Wu, Multiobjective optimum design of a 3-RRR spherical parallel manipulator with kinematic and dynamic dexterities, *Model. Identif. Control* 33 (3) (2012) 111–122.
- [74] J. Wu, Z. Yin, A novel 4-DOF parallel manipulator H4, in: H. Wu (Ed.), *Parallel Manipulators, Towards New Applications*, I-Tech Education and Publishing, Vienna, Austria, 2008, p. 506. April.